

Thermal Grooving in 3% Silicon-Iron

R. L. COLOMBO*, J. HOWARD†

Division of Materials Applications, National Physical Laboratory, Teddington, Middlesex, UK

Received 6 January 1969

The grain-boundary grooving technique has been used to determine the transport mechanism and the grain-boundary energies in randomly oriented and in textured 3% silicon-iron strips. The matter transport mechanism was found to be mainly volume diffusion, and the calculated diffusion coefficient was:

$$D_m = 0.15 \exp [- (47\,500 \pm 6300)/RT]$$

The average energy of incoherent large-angle grain-boundaries is shown to be 0.37 times the surface energy at 1150° C and 0.30 times at 1250° C: the difference is tentatively explained in terms of oxygen absorption and the contribution of evaporation condensation to the transport mechanism. Results from textured specimens suggest that all incoherent large-angle boundaries have approximately the same energy per unit surface. Lower energies are typical of low-angle boundaries and of coincident-site boundaries containing a sub-boundary consisting of a few dislocations.

1. Introduction

Thermal grooving at grain-boundaries has been known for more than half a century [1] and the first explanation was put forward soon after its discovery. However, the conditions for the occurrence of such a phenomenon and its relationships with surface and grain-boundary energies were not established until much later [3, 4].

If 1 and 2 are two adjoining grains of a metal or alloy, whose free surfaces meet at angle θ_{12} (fig. 1), and if the angles between these free surfaces and the grain-boundary are respectively θ_1 and θ_2 , then [2] as long as Herring's "torque terms" can be neglected the following relationships exist among the surface free energies, γ_{s1} and γ_{s2} , and the grain-boundary energy γ_b per unit area:

$$\gamma_b / \sin \theta_{12} = \gamma_{s1} / \sin \theta_2 = \gamma_{s2} / \sin \theta_1 \quad (1)$$

Since in most experimental cases one is justified in assuming that $\gamma_{s1} = \gamma_{s2} = \gamma_s$ and, moreover, $\theta_1 = \theta_2$, equation 1 simplifies to

$$\gamma_b = 2\gamma_s \cos \theta \quad (2)$$

where θ is half the dihedral angle θ_{12} and is usually about 80°.

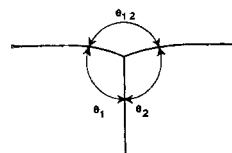


Figure 1 Equilibrium angles at a grain-boundary groove (schematic).

A number of workers (reviewed in [3, 4, 5]) have used thermal grooving and scratch-flattening to determine surface and grain-boundary energies and the mechanism of matter transport. Under the conditions usually met, the width w and the depth d (fig. 2) of a groove established at a grain-

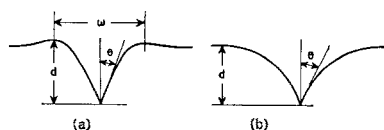


Figure 2 Grain-boundary groove: (a) diffusion controlled; (b) evaporation-condensation controlled (schematic, vertical scale largely exaggerated).

boundary, after annealing at temperature (absolute) T for a time t , can be calculated mathe-

*Guest scientist from the Centro Sperimentale Metallurgico, Rome, Italy.

†Now at PO Research Station, Dollis Hill, NW2.

matically. Let p_0 be the equilibrium vapour pressure at a flat surface, D_s the surface self-diffusion coefficient, D_m the volume mass transfer self-diffusion coefficient (which differs from the volume self-diffusion coefficient to take into account the lattice correlation factor and the possibility that the material under study is not monatomic), M the mass of the molecule evaporating from the surface, Ω the molecular volume, ν the surface atomic density and k the Boltzmann constant; then providing that the grain-boundary does not act either as a "source" or "sink" of material, and that θ is close to 90°

$$w = 4.6 (D_s \gamma_s \Omega^2 \nu / kT)^{1/4} t^{1/4}, \quad (3)$$

$$d = 0.973 (\gamma_b / 2\gamma_s) (D_s \gamma_s \Omega^2 \nu / kT)^{1/4} t^{1/4}, \quad (4)$$

for surface diffusion;

$$w = 5 (D_m \gamma_s \Omega / kT)^{1/3} t^{1/3}, \quad (5)$$

$$d = 1.01 (\gamma_b / 2\gamma_s) (D_m \gamma_s \Omega / kT)^{1/3} t^{1/3}, \quad (6)$$

for volume diffusion;

$$d = 1.13 (\gamma_b / 2\gamma_s) [p_0 \gamma_s \Omega^2 / (2\pi M)]^{1/2} (kT)^{3/2}]^{1/2} t^{1/2} \quad (7)$$

for evaporation-condensation. The twin "hills", which run parallel to the groove, are predicted by the theory when the transport mechanism is diffusion (whether surface or volume), but not when it is evaporation-condensation. In practice, it would be expected that all three mechanisms contribute to the formation of grain-boundary grooves. However, with the possible exception of chromium annealed *in vacuo* [6] the contribution of evaporation condensation has always been thought to be negligible.

In the present work, new estimates are made for 3% silicon-iron of the variation of relative grain-boundary energies with misorientation in randomly oriented and textured test pieces. From measurements of the changes in the grain-boundary groove width with time an estimate of the volume self diffusion coefficient has been obtained.

2. Experimental Procedure

2.1. Materials

The 3% silicon-iron alloy was produced by the method of Hopkins *et al* (*J.I.S.I.* **168** (1951) 377).

The alloy was chill cast into a 10 cm octagonal mould and the ingot hot rolled into 12.5 mm thick sheet. The chemical analysis of a typical

specimen after the experimental work was carried out is given in table I.

TABLE I Chemical composition (%) of a typical specimen

| Silicon | 2.95 |
|------------|----------------|
| Carbon | 0.002 |
| Sulphur | 0.0002 |
| Phosphorus | 0.0037 |
| Arsenic | 0.001 |
| Aluminium | 0.0015 |
| Cobalt | 0.004 |
| Copper | 0.0035 |
| Chromium | < 0.0005 |
| Manganese | 0.001 |
| Molybdenum | 0.002 |
| Nickel | 0.005 |
| Nitrogen | 0.0009 |
| Oxygen | not determined |

The experimental work was carried out in a recrystallised alumina tube furnace, through which was passed a stream of specially purified hydrogen.

When the furnace was cold the dew point of the hydrogen was between -75 and -80°C , but at higher temperatures it inevitably rose owing to the porosity of the alumina tube.

However, all the results quoted in the following have been obtained with dew points of -42°C or better.

2.2. Randomly Oriented Material

The 12.5 mm thick material was annealed *in vacuo* and then cold rolled to 1 mm approximately. To obtain stabilised grains, sheet specimens were annealed for 60 h at 1325°C in dry hydrogen. At this point it was ascertained that the grain-boundaries ran perpendicularly to the rolled surface. A further 20 h at 1330°C was then given to ensure that no more grain growth took place. In this way three suitable sheet specimens were produced. The orientations of the individual crystals used in the experiments were determined by the etch-pit technique described by Barrett [7], the accuracy of the measurements being of the order of $\pm 1^\circ$. With few exceptions, the normals to the surface plane of each crystal were sufficiently far from the poles of the nearest $\{100\}$, $\{110\}$ and $\{111\}$ planes (i.e. the planes most likely to be those with the minimum energies), to justify the assumption of an average value for the

surface energy of all the crystals in the surface.

The orientations of two neighbouring crystals in one of the specimens were found to be related by a rotation of some 60° measured about $\{111\}$ axis, corresponding to a twin relationship.

2.3. Textured Material

The so-called "strip thickness inhibition" method [8], by which the formation of either $\{110\}$, $\{001\}$ or $\{100\}$, $[001]$ textures is controlled by surface energy was used to produce the textured specimens.

The sheets intended to provide the textured material were obtained by cold rolling from 12.5 mm by small percentage reductions (25 to 50%) and high temperature intermediate anneals (1150 to 1250° C) to final thicknesses of 0.38 to 0.76 mm.

The stabilising anneals for the $\{100\}$ texture were at 1200° C followed by 1300° C and for the $\{110\}$ texture at 1300° C only; one specimen of the former and three of the latter were produced. The Barrett technique was again used to determine the angles of mismatch about the axis normal to the rolling surface of the adjoining crystals. Since the $\{110\}$ and $\{100\}$ planes were very near, but in general not exactly in the rolling surface, the figures for the smaller angles of mismatch are proportionally less accurate than those for the larger ones.

2.4. Grain-Boundary Grooving

In order to develop thermal grooves at the grain-boundaries, the specimens were first polished mechanically and then electrolytically to remove all traces of any grooves previously produced. They were then given a series of anneals for different times at different temperatures. The temperatures were measured and maintained within $\pm 2^\circ$ C of the indicated value. Since the shortest annealing time was 5 h, no account has been taken of the heating up and cooling down periods.

Observation of the annealed specimens was carried out using a Hilger & Watts interferometric microscope of the Linnik type. In the preliminary experiments at about 1300° C, the specimens were laid flat on a sheet of pure recrystallised alumina. This method resulted in a large number of grain-boundaries slipping, as well as developing grooves, as can be seen in fig. 3. Such slipping was significantly reduced if the specimens were supported during heat-treatment by hanging them between a U-

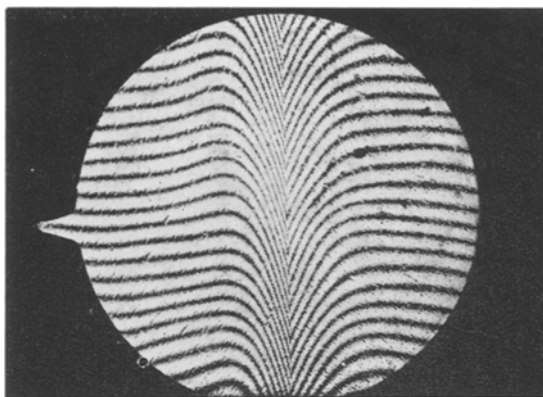


Figure 3 Grain-boundary slipping (interferometric micrograph, horizontal magnification: $\times 280$).

shaped piece of silicon-iron taken from the same strip as that from which the specimen was taken. It was concluded that the slipping was due mainly to shear creep parallel to the vertical grain-boundary, i.e. produced by gravity. For a crystal of 3 mm diameter, the stress would be roughly 6×10^8 dynes/cm².

Fig. 4, shows a very good grain-boundary groove perfectly symmetrical on both sides. In cases where a very small amount of asymmetry had to be accepted, the depth of the groove was given as the arithmetic average of the figures measured from either side. If the asymmetry was marked the grain-boundary was not used.

While at dew points of -55° C or lower very little oxidation appeared under the optical microscope, isolated oxidation nuclei with a

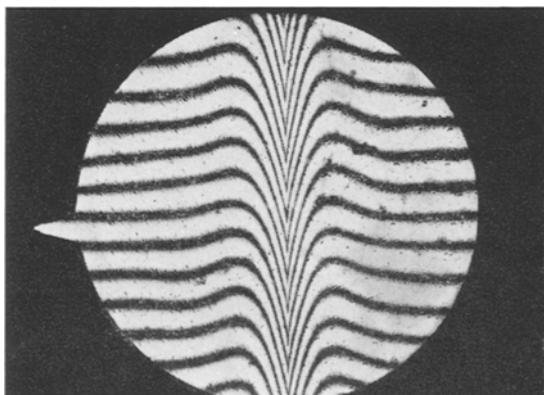


Figure 4 Symmetric groove (interferometric micrograph, horizontal magnification: $\times 280$).

marked epitaxial character were visible at higher dew points. However, it was assumed that as long as they remained isolated the ratio of the surface to the grain-boundary free energy would not be significantly affected.

3. Results and Discussion

3.1. Transport Mechanism

The width of the grooves, which is easier to measure than the depth, was used to determine the transport mechanism. Randomly oriented specimens were preferred because of the higher number of suitable grain-boundaries that they provided and the larger variety of orientations which were available. The solid lines of fig. 5 represent plots of w against t at temperatures from about 1100 to 1300° C for such specimens, each point being the average of several measurements made on different boundaries.

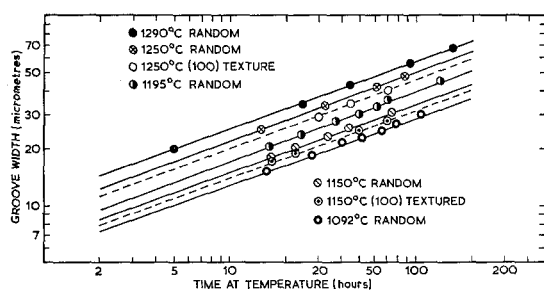


Figure 5 Variation of the groove width with heat-treatment

The broken lines represent boundaries between crystals having $\{100\}$ planes in their surfaces. Even though the scatter is apparently larger, the same slope as that of the corresponding solid lines can reasonably be assumed. The solid lines are above the dotted lines for the same temperature owing, probably, to the lower surface energy of the $\{100\}$ planes.

Figures for the slopes of the linear plots at each temperature are given in table II. The average value is 0.350 ± 0.008 , but a consistent increase in slope with temperature, whether significant or not, is apparent.*

If this increase of slope with temperature is significant, it might be due to the adsorption of some highly surface-active impurities (probably oxygen) from the atmosphere so that γ_s would be higher at higher temperatures. It is believed that the contribution of surface diffusion (theoretical

*All errors given at ± 1 standard deviation

TABLE II Slopes of the log w against t lines at various temperatures

| Temperature ° C | Slope |
|-----------------|-------------------|
| 1092 | 0.341 ± 0.015 |
| 1150 | 0.348 ± 0.006 |
| 1195 | 0.348 ± 0.008 |
| 1250 | 0.354 ± 0.004 |
| 1290 | 0.362 ± 0.007 |

slope: 0.25) to matter transport is negligible, but some contribution from evaporation-condensation cannot be excluded although its effect on w is thought to be small. It is concluded that by far the most important mechanism operative in this case is volume diffusion (theoretical slope: 1/3). The rest of the calculations have been carried out in accordance with equation 5, assuming an average value of 2000 ergs/cm² for γ_s (neglecting its dependence on temperature) and taking $\Omega = 1.17 \times 10^{-23}$. The calculated diffusion coefficients at each temperature are given in table III, and are, as would be expected, in the 10^{-8} range.

TABLE III Diffusion coefficients at various temperatures

| Temperature ° C | Diffusion coefficient cm ² /sec $\times 10^8$ |
|-----------------|---|
| 1092 | 0.411 |
| 1150 | 0.678 |
| 1195 | 1.113 |
| 1250 | 2.618 |
| 1290 | 3.390 |

The least squares Arrhenius plot gives

$$D_m = (0.15) \exp [-(47500 \pm 6300)/RT]$$

Table IV shows that the figures for the activation energy Q agree with others existing in the literature within experimental error. The pre-exponential factor D_0 is of the same order of magnitude as the radioactive tracer value, but is smaller than the others. It is believed that the overall agreement with results obtained in different experiments is reasonable and indirectly justifies the choice of the time exponent.

The results agree with previous work [9, 12], leading to the conclusion that in silicon-iron matter transport is predominantly through volume diffusion. Young and Mykura [13] found

TABLE IV Volume diffusion coefficients in silicon-iron.

| Silicon % | Technique | D_0 cm ² /sec | Q cal/mol | References |
|-----------|-----------------------|----------------------------|---------------|------------------------|
| 3.8 | scratch annealing | 2.3 | 53 000 ± 3500 | Blakely and Mykura [9] |
| 3.0 | radiotracer | 0.44 | 52 200 ± 3000 | Mills et al [10] |
| 3.5 | Herring-Nabarro creep | 4.3 | 56 000 ± 6000 | Hondros [11] |
| 3.0 | thermal grooving | 0.29 | 47 485 ± 6300 | This work |

that in pure α -iron annealed up to 880° C surface diffusion was the prevailing mechanism, while extrapolation of existing data indicates that it would still be so if α -iron were stable up to the melting point [14]. Furthermore, measurements on grain-boundary grooving kinetics at 955° C in 3% silicon-iron mentioned by Mills, Jones, and Leak [12] show that surface diffusion is two orders of magnitude slower in the alloy than in the pure metal. In gold, oxygen was found to suppress surface diffusion in favour of volume diffusion [15]. This does not seem to happen in pure iron and the reason why it may occur in silicon-iron despite the extremely small amount of oxygen in the annealing atmosphere, is tentatively explained as follows. Surface diffusion [16] is presumably related to the adherence of adatoms on top of the metal surface, which subsequently grow into expanding terraces. When a terrace has become wide enough another adatom can adhere on top of it and so on. According to Hondros and Stuart [17] the silicon surface enrichment in 3% silicon iron at 1410° C is about 10% and so the probability that a silicon atom is at the edge of an expanding terrace is quite high. If it is assumed that a silicon atom in such a position is extremely reactive and can pick up an oxygen atom whenever it exists in the atmosphere, then the extremely low solubility of oxygen in iron will prevent any further expansion of the terrace. If this happens while the terrace is still too narrow for an adatom to adhere on top of its surface, diffusion is suppressed altogether in a way similar to the well-known impurity poisoning of crystal growth.

3.2. Grain-Boundary Energies

Equations 5 and 6 give by division:

$$\gamma_b/\gamma_s = 9.90 d/w \quad (8)$$

so that the ratio of the free energy of a grain-boundary to the surface free energy can be obtained directly from the measurements of the depth and width of the groove. Measurements taken at different stages of development of the same groove always yielded the same ratio with

very good consistency. All the data quoted in the following were obtained from specimens which had undergone the longest anneal at each temperature. The method described above is much quicker than the direct measurement of the dihedral angle and should not be much less accurate. It was therefore adopted throughout the present work.

Fig. 6 shows the γ_b/γ_s against ϕ plots at 1100 and 1200° C for boundaries between randomly oriented crystal specimens, the mismatch angles indicated being the lowest measurable, regardless of the axis of rotation.

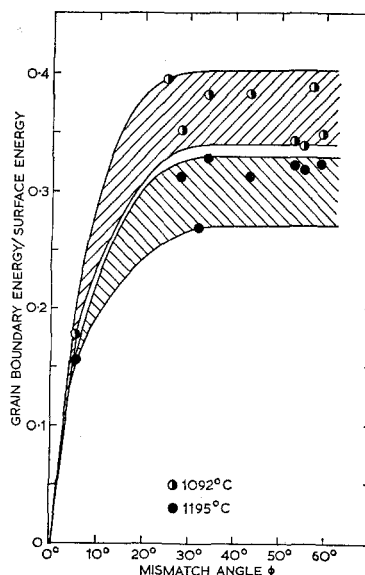


Figure 6 Dependence of grain-boundary energy on mismatch angle between crystals for randomly oriented specimens.

The average ratio of the large-angle incoherent boundary energy to the surface energy is about 0.37 at 1100° C and 0.30 at 1200° C. In table V such data are given together with those taken from the literature and show agreement. The large difference in the γ_b/γ_s ratio at 1100 and 1200° C is not easily explained. Since γ_b is not

TABLE V Grain-boundary energies in bcc iron and alloys.

| Specimen material | Shape | Temperature °C | Atmosphere | Technique | γ_b erg/cm ² | γ_b/γ_s | References |
|-------------------------|-------|----------------|-------------------------------|-------------------------------------|--------------------------------|---------------------|-------------------------|
| 4% Si-0.2% C-0.26% S-Fe | bulk | 1105 | — | dihedral angle between phases | 760 | — | Van Vleck [18] |
| α -Fe | strip | 880 | 10 ⁻⁵ Torr vacuum | grain-boundary grooving | — | 0.48 | Blakely and Mykura [9] |
| δ -Fe | wire | 1405-1515 | argon | dihedral angle by grooving in creep | 470 | 0.24 | Price <i>et al</i> [19] |
| δ -Fe | sheet | 1450 | dry H ₂ | same | 795 | 0.38 | Hondros [20] |
| 0.044-0.35% P-Fe | sheet | 1450 | dry H ₂ | same | 755-410 | 0.35 | same |
| 2.9% Si-Fe | wire | 1275-1445 | nitrogen | same | 530 | 0.32 | Jones and Leak [21] |
| 0.01% N-Fe | sheet | 1400-1500 | nitrogen + 10% H ₂ | same | 660 | 0.35 | Hondros [22] |
| 3% Si-Fe | sheet | 1330 | - 50° C dew point hydrogen | same | 462 | 0.24 | Hondros and Stuart [17] |
| 3% Si-Fe | sheet | 1330 | - 20° C dew point hydrogen | same | 496 | 0.324 | same |
| 3% Si-Fe | strip | 1150 | dry H ₂ | grain-boundary grooving | — | 0.37 | this work |
| 3% Si-Fe | strip | 1250 | dry H ₂ | grain-boundary grooving | — | 0.30 | same |

expected to be influenced greatly by the temperature, the effect might be ascribed to the absorption of oxygen at the lower temperature which would decrease γ_s , though the increase of the surface energy on desorption would probably be too high. Another contribution might come from the concurrence of evaporation-condensation and the transport mechanism since the activation energy for evaporation is higher than that for diffusion.

A ratio of twin to large-angle boundary was derived from this work to be 0.3, while Blakely and Mykura [9] find 0.25 and Dunn, Daniels and Bolton [23] find 0.22.

Fig. 7 shows the γ_b/γ_s against ϕ plot for textured specimens. The mismatch angles in this case are for rotations about the nominal axis normal to the plane of the surface. Unfortunately data are much more abundant for low-angle than large-angle (tilt) boundaries, as the textures tend to be doubly oriented. The data are tentatively represented by lines in the figure bearing in mind the degree of symmetry of the axis of rotation and the fact that a twin occurs at equilibrium for a rotation of some 70° about a $\langle 110 \rangle$ axis (actually no such twin was found in the textured specimen, and the twin energy has been assumed to be 0.15 times the $\{110\}$ surface

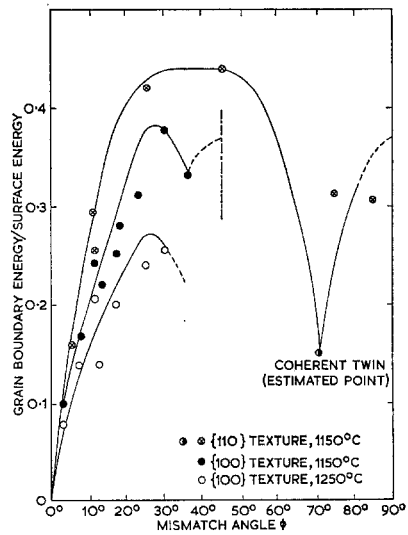


Figure 7 Dependence of grain-boundary energy on mismatch angle between crystals for textured specimens.

energy). The line representing the $\{110\}$ textured specimen correctly runs higher than that representing the $\{100\}$ specimen annealed at the same temperature.

For the $\{100\}$ specimens data are available at

1250° C and again the line at higher temperature runs lower. Whatever the reason for the phenomenon, the pattern of the grain-boundary energy against mismatch angle should not be affected, and a comparison can be established between the present results and those by Dunn and Lionetti [24], and Dunn, Daniels, and Bolton [23] (figs. 8 and 9).

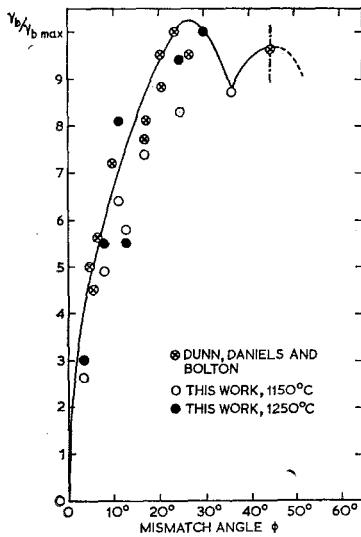


Figure 8 Comparison of data from the literature for grain-boundary energy in silicon-iron {100} texture.

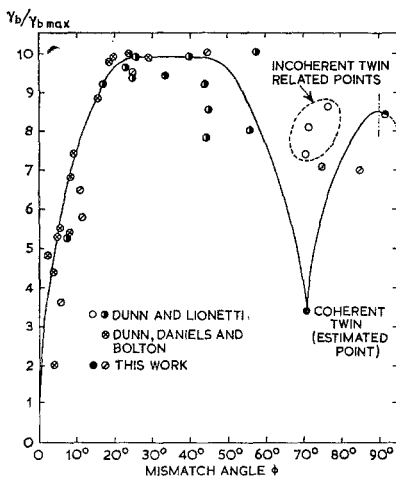


Figure 9 Comparison of data from the literature for grain-boundary energy in silicon-iron: {110} texture.

It is believed that, within experimental uncertainties, all incoherent large-angle boundaries have the same free energy per unit surface.

Lower energies are typical of less incoherent boundaries, viz. (i) low-angle dislocation boundaries, (ii) low-order csb's and (iii) boundaries which can be described as the sum of a low order csb and superimposed sub-boundary made of few enough dislocations.

Acknowledgement

The authors are indebted to a number of their colleagues of the National Physical Laboratory, who have helped them with fruitful suggestions, and discussions: in particular, Dr D. McLean, Dr E. D. Hondros and Mr J. Rendall.

References

1. W. ROSENHAIN and J. W. C. HUMFREY, *Proc. Roy. Soc.* **83A** (1910) 200.
2. C. HERRING, "Structure and Properties of Solid Surfaces" edited by R. Gomer and C. S. Smith (University of Chicago Press, 1952).
3. W. W. MULLINS, in "Metal Surfaces: Structure, Energetics and Kinetics" (ASM, Metals Park, Ohio, 1963).
4. J. M. BLAKELY, *Progr. Materials. Sci.* **10** (1963) 394.
5. W. W. MULLINS, *J. Appl. Phys.* **28** (1957) 333.
6. E. B. ALLAN, *Trans AIME* **236** (1966) 915.
7. C. S. BARRETT, in "The Structure of Metals" (McGraw Hill, New York, 1948).
8. K. DETERT, *Acta Metallurgica* **7** (1959) 589.
9. J. M. BLAKELY and H. MYKURA, *ibid* **11** (1963) 389.
10. B. MILLS, G. C. WALKER, and G. M. LEAK, *Phil. Mag.* **12** (1965) 939.
11. E. D. HONDROS, *Phys. Stat. Sol.* **21** (1967) 375.
12. B. MILLS, H. JONES and G. M. LEAK, *Met. Sci. J.* **1** (1967) 9.
13. W. S. YOUNG and H. MYKURA, *Acta Metallurgica* **13** (1965) 449.
14. B. MILLS, Ph.D Thesis, University of Manchester (1966).
15. J. M. BLAKELEY, *Trans. Faraday Soc.* **57** (1961) 1164.
16. J. Y. CHOI and P. G. SHEWMON, *Trans. AIME* **224** (1962) 589.
17. E. D. HONDROS and L. E. H. STUART, *Phil. Mag.* **17** (1968) 711.
18. L. H. VAN VLECK, *Trans. AIME* **101** (1951) 251.
19. A. T. PRICE, H. A. HALL, and A. P. GREENHOUGH, *Acta Metallurgica* **12** (1964) 49.
20. E. D. HONDROS, *Proc. Roy. Soc.* **286A** (1965) 479.
21. H. JONES and G. M. LEAK, *Acta Metallurgica* **14** (1966) 21.
22. E. D. HONDROS, *Met. Sci. J.* **1** (1967) 36.
23. C. G. DUNN, F. W. DANIELS, and M. J. BOLTON, *Trans. AIME* **188** (1950) 368; *ibid* 1245.
24. G. S. DUNN and LIONETTI, *ibid* **184** (1949) 125.